Journal of Nuclear Materials 437 (2013) 359–364

Contents lists available at SciVerse ScienceDirect

Journal of Nuclear Materials

journal homepage: www.elsevier.com/locate/jnucmat

Hydrogen yields from water on the surface of plutonium dioxide

Howard E. Sims [a,*], Kevin J. Webb [b], Jamie Brown [b], Darrell Morris [c], Robin J. Taylor [b,*]

[a] National Nuclear Laboratory, Harwell Science Park, Didcot, Oxon OX11 0QT, UK
[b] National Nuclear Laboratory, Central Laboratory, Sellafield, Seascale CA20 1PG, UK
[c] Nuclear Decommissioning Authority, Herdus House, Westlakes Science and Technology Park, Moor Row, Cumbria CA24 3HU, UK

HIGHLIGHTS

- Hydrogen evolution due to water radiolysis on samples of Sellafield PuO_2.
- Sharp increase in hydrogen evolution above 75% relative humidity.
- Hydrogen evolution due to radiolytic rather than thermal reaction.
- Analysis of trends from literature data.

ARTICLE INFO

Article history:
Received 6 October 2012
Accepted 15 February 2013
Available online 27 February 2013

ABSTRACT

The long term storage of separated plutonium dioxide (PuO_2) in sealed canisters requires an understanding of the processes occurring within the cans. This includes potential mechanisms that lead to can pressurisation, including the radiolysis of adsorbed water forming hydrogen. New measurements of H_2 production rates from three sources of PuO_2 show low rates at low water monolayer coverage but a sharp increase between 75% and 95% relative humidity. This behaviour being quite different to that reported for CeO_2 and UO_2, which, therefore, cannot be considered as suitable analogues for PuO_2/H_2O radiation chemistry. It is concluded that surface recombination reactions are likely to be important in the radiation chemistry and that the H_2 production arises from a radiolytic process and not a thermal reaction, at least in these experiments.

1. Introduction

There is a large amount of plutonium dioxide (PuO_2) in storage around the world, including a large stockpile at the Sellafield site (United Kingdom). The vast majority of UK PuO_2 is derived from reprocessing of spent uranium metal fuels from UK Magnox reactors ("Magnox" PuO_2) or reprocessing of spent oxide fuels from UK Advanced Gas Cooled reactors or foreign light water reactors in the Thorp reprocessing plant ("Thorp" PuO_2). The UK stockpile has accumulated over the last ~50 years. The UK Government is now considering eventual re-use of this Pu as mixed oxide fuel for thermal reactors [1,2]. Current "Magnox" PuO_2 product is contained in an aluminium screw top container, inside a polyethylene (PE) bag and contained in a welded outer steel container. Similarly, "Thorp" PuO_2 is contained in a stainless steel screw top inner can held within a vented intermediate can placed inside a welded outer container. Conditions are carefully controlled during production and packaging to limit water adsorption into the PuO_2 powder and to meet acceptance criteria for storage (e.g. specific surface area). Very similar arrangements have been adopted by the United States Department of Energy (DOE) for storing US PuO_2, as described in the DOE 3013 standard [3].

Of thousands of cans in stores only a few "out-of-specification" cans containing very wet material are known to have pressurised. This empirically vindicates the acceptance criteria specified for storage. Even so, this is perhaps surprising because PuO_2 adsorbs water up to many monolayers and it might be expected that this water would be radiolysed to hydrogen and oxygen, thus pressurisation should be observed even for cans that meet specifications for water content (*via* LOH: Loss on Heating measurements). It is highly unlikely that at these high dose rates, typically 8 W kg^{-1}, radiolysis does not occur so it must be assumed that a reverse reaction, such as recombination of radiolysis products on the surface of PuO_2, also occurs. Little is known about either process, although there are other reports of hydrogen production from PuO_2 [4–6] and can pressurisation was reported at Harwell nearly 50 years ago [7].

Abbreviations: DOE, (US) Department of Energy; GC, gas chromatography; LOH, Loss on Heating analysis; PE, polyethylene; RH, Relative Humidity; SSA, specific surface area.

* Corresponding authors. Tel.: +44 19467 79266; fax: +44 19467 79007.
E-mail addresses: howard.e.sims@nnl.co.uk (H.E. Sims), robin.j.taylor@nnl.co.uk (R.J. Taylor).

0022-3115/$ - see front matter © 2013 Elsevier B.V. All rights reserved.
http://dx.doi.org/10.1016/j.jnucmat.2013.02.040

Table 1
SSA of PuO_2 samples.

Sample	SSA ($m^2\ g^{-1}$)	Specific activity (Bq-$\alpha\ g^{-1}$ Pu)	MeV (total) ($s^{-1}\ g^{-1}$ Pu)
Magnox	8.9 ± 1.1	5.5×10^9	2.9×10^{10}
Thorp	6.1 ± 1.0	1.8×10^{10}	9.6×10^{10}
Ex-LOH	2.1 ± 0.8	6.1×10^9	3.1×10^{10}
Slurry samples	8.9 ± 1.1	5.2×10^9	2.8×10^{10}

Although the vast majority of cans do not pressurise, it is clear that there is a considerable amount of chemistry occurring within them [8]. In "Magnox" PuO_2 cans N_2 and O_2 are radiolysed initially to oxides of nitrogen and PE undergoes thermal and radiolytic reactions which adsorb oxygen. The result is that some cans actually depressurise initially. "Thorp" PuO_2 is stored under argon with a metal intermediate can rather than a PE bag so neither of these mechanisms applies. Due to its higher specific activity, "Thorp" PuO_2 self heats to higher temperatures and develops higher pressures from He production. Furthermore, there is still controversy as to whether PuO_2 can thermally react with H_2O to form PuO_{2+x} and H_2 [9]. Note also that during prolonged storage the morphology of the PuO_2 is expected to change as ^{241}Pu decays to ^{241}Am, He from alpha decay builds up and is gradually evolved into the gas phase and radioactive decay products damage the PuO_2 lattice [10].

So whilst there is plenty of operational experience in the safe and secure storage of PuO_2 in sealed canisters on nuclear licensed sites, there remains a clear need to underpin storage through better understanding of the fundamental chemical and physical processes occurring within the storage cans. Improved scientific understanding can also reduce some of the pessimisms built into stores' safety cases giving operational benefits such as allowing wider package specifications or extended package lifetimes.

In work described in this report, production line samples of "Thorp" and "Magnox" PuO_2 were used to provide material with different specific activities and specific surface areas (Table 1). Both plants use the oxalate conversion route with calcination at ~600 °C leading to variations in SSA [11]. Also a "Magnox" PuO_2 sample that had been used for measurement of weight changes from heating (LOH analysis) was used. As this material had been heated to >950 °C the specific surface area was substantially reduced due to partial sintering causing closure of pores with consequent loss in porosity and morphological changes [11]. These three samples thus provide variations in the number of monolayers of water that will be adsorbed onto the PuO_2 and the energy (dose) transferred to the adsorbed water molecules, the key factors that should determine radiolytic yields of H_2. Also a range of relative humidities (RHs) were studied from 0% to 95%. All experimental work was carried out at room temperature.

2. Experimental methods

2.1. Overview

Four different sources of PuO_2 samples were obtained for study:

- "Magnox" PuO_2 (denoted M).
- "Thorp" PuO_2 (T).
- Ex-Loss on Heating PuO_2 (L) – a sample of "Magnox" PuO_2 production material heated to ~950 °C during routine LOH analysis (to check product quality) thus altering morphology and reducing specific surface area (SSA), and
- Second sample of "Magnox" PuO_2 used for slurry experiments (S).

Samples were dried and then equilibrated in atmospheres with a range of relative humidity from 0% to 95% with intermittent weighing to confirm hydration levels. Samples were labelled M*X*, T*Y* or L*Z* to represent the material type and the degree of humidity to which they were exposed. For example, M95 denotes "Magnox" PuO_2 exposed to 95% humidity and L*D* for Loss on Heating "Magnox" PuO_2 that has been kept dry, i.e. exposed to 0% humidity. Two experiments using slurries of PuO_2 were labelled S and SN, the N denoting nitrite doping. Finally, gas samples were taken at intervals and analysed for H_2. Three series of measurements were taken to enable an average H_2 evolution rate to be calculated. The atmosphere in the irradiation vessels was completely refreshed to remove evolved hydrogen between each series. Further experimental details are given below.

2.2. Plutonium oxide samples

The specific surface area (SSA) and specific activity (alpha) for each of the samples are given in Table 1 and the isotopic composition in Table 2.

Approximately 0.4–1.0 g of PuO_2 powder was used in these experiments. All of the samples were 'dried' for 30 days prior to the experiment by storing in desiccators. Initially calcium sulphate anhydrite, $CaSO_4{\cdot}nH_2O$ (where n = 0–0.05), was used as a desiccant. Half-way through the drying period the desiccant was changed to phosphorus pentoxide (P_2O_5) to further improve the drying process. The mass of each sample was recorded at intervals through the drying period to check progress. It is assumed that two monolayers of water were not removed during the drying process, one being chemisorbed to the PuO_2 surface and a second being physisorbed to the first. Similarly, Stakebake and Steward [12] reported three monolayers of water on PuO_2 which had been repeatedly equilibrated with water vapour and dried.

At the end of the drying process the samples were transferred to a vessel with a controlled atmosphere to equilibrate with a humid atmosphere. For the samples which required equilibrating at 25%, 50%, 75% and 95% Relative Humidity (RH), the appropriate molarity of sulphuric acid based on literature information was used to generate the RH required [13].

The slurry samples (~0.05 g PuO_2) were treated differently in that they were mixed with deionised water (~1 mL), sample SN also being doped with 2 mM sodium nitrite solution.

The sample vessel for the radiolysis experiments consisted of two parts: a small glass "inner vessel" which held the plutonium dioxide, and an "outer vessel" of a quickfit test tube which held the drying agent or sulphuric acid. The quickfit test tubes were fitted with a vacuum rated valve to enable gas samples to be removed for analysis.

The quickfit test tube was first loaded with the drying agent or sulphuric acid then with the tube containing PuO_2. The valves were placed on the tubes but were initially left open so that hydrogen associated with the samples could escape. Once all the vessels were filled with drying agent/sulphuric acid and PuO_2, the vessels were carefully agitated and evacuated to 0.1 bar using a hand pump to further remove hydrogen before back filling with air. A further evacuation to 0.1 bar was undertaken to leak test the equipment plus ensure complete removal of hydrogen gas associated with the PuO_2. The vessel was then back filled with air before shutting the valve.

Table 2
Isotopic composition of the PuO_2 samples used.

Isotope fraction	Magnox	Thorp	Ex-LOH	Slurry (Magnox)
Pu-238	0.0025	0.0217	0.0028	0.0025
Pu-239	0.7119	0.5379	0.6935	0.7119
Pu-240	0.2341	0.2862	0.2505	0.2341
Pu-241	0.0373	0.0745	0.0377	0.0390
Pu-242	0.0119	0.077	0.0131	0.0119
Am-241	0.0023	0.0026	0.0023	0.0006

2.3. Hydrogen analysis

The gas in each experiment was periodically sampled (typically 10 mL from ~63 mL head space) by using a gas syringe connected to the valve on the sample vessel. The gas sample was analysed for hydrogen using an Agilent 3000 micro gas chromatograph (GC). The experiments were typically run for at least 5 days with periodic sampling and analysis. The Agilent 3000 micro GC was calibrated using standardised 100 ppm hydrogen in argon prior to use and checked against the same standard on completion of the set of samples. At and above 100 ppm the variation on the analysis was within a few percent but possibly 10 s of percent around the 10 ppm hydrogen level. The gas samples were analysed within 4 h of sampling and hydrogen loss due to this is estimated at a no more than ca. 5%. (Note the complete analytical procedures were tested using standardised concentrations of H_2 prior to experiments with Pu).

In all cases hydrogen concentrations were plotted as a function of time and hydrogen production increased linearly with time. GH_2 values (the number of molecules of hydrogen formed per 100 eV energy deposited in solution, molec. 100 eV^{-1}) were calculated from the gradients of the H_2 *vs.* time graphs.

3. Results

The numbers of monolayers measured from weight changes after 22 days of equilibration are shown for each RH in Fig. 1. H_2 production rates are shown in Table 3. These are taken from the gradients of graphs of H_2 production rate *vs.* time; a typical example is given in Fig. 2. Generally, better agreement was observed between the second and third datasets which may be due to some stabilisation of the experimental system.

A noteworthy feature of the data is that in all cases the hydrogen production rate increased by an order of magnitude on increasing RH from 75% to 95% whereas the number of monolayers of water (assuming two on the "dry" sample) increased by about a factor of around three.

4. Discussions

4.1. Dosimetry

For radiation chemistry applications the *G*-value is used where in this case GH_2 is defined by the following equation:

$$GH_2 = \frac{\text{molecules } H_2}{100 \text{ eV}} \quad (1)$$

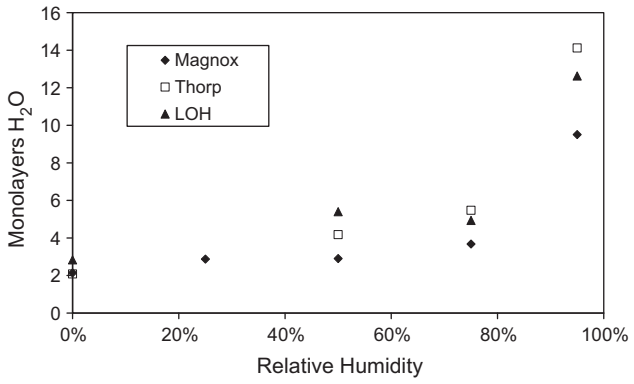

Fig. 1. Number of calculated monolayers of water *vs.* Relative Humidity (%) for Magnox, Thorp and low SSA ("LOH") PuO_2 samples (note: assumes two monolayers still present after room temperature drying in desiccators).

Table 3
H_2 production rates.

Sample	H_2 production rate (cm^3 day^{-1} g PuO_2^{-1})		
	Run 1	Run 2	Run 3
MD	5.75E-06	7.28E-06	Not run
M25	1.56E-05	2.08E-05	2.27E-05
M50	2.98E-05	3.69E-05	3.72E-05
M75	7.14E-05	5.99E-05	6.82E-05
M95	6.51E-04	7.21E-04	7.12E-04
TD	9.99E-06	7.43E-06	1.32E-05
T50	4.41E-04	6.38E-05	7.22E-05
T75	1.18E-04	1.76E-04	2.08E-04
T95	1.76E-03	2.05E-03	2.10E-03
LD	5.85E-06	3.87E-06	5.12E-06
L50	7.19E-06	7.75E-06	1.24E-05
L75	9.65E-06	1.54E-05	1.69E-05
L95	1.41E-04	1.58E-04	1.64E-04
S	0.019 (Average of all data)		
SN	0.022 (Average of all data)		

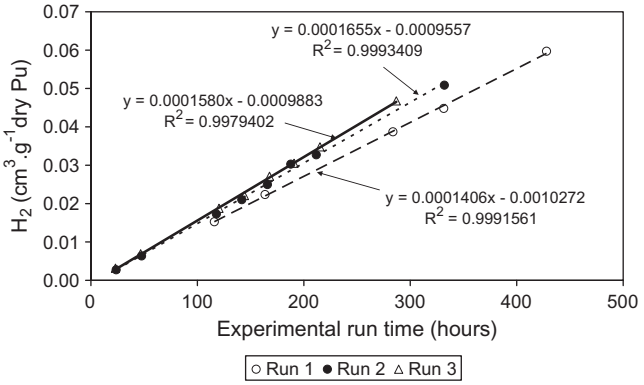

Fig. 2. An example of H_2 yields (cm^3 per gram of dry PuO_2) *vs.* time for a typical sample (sample L95, i.e. LOH PuO_2, 95% RH). Data represents three separate runs under the same initial conditions.

In order to make comparisons with other radiation chemical yields (*G*-values) it is important to estimate the fraction of dose into the water. For a specific surface area of 2–10 m^2 g^{-1} the equivalent particle size must be very small and much less than the range of 5.5 MeV $^4He^{2+}$ in PuO_2 (12.5 μm) so we can make a simplifying assumption that the water is homogeneously distributed through the PuO_2. Normally radiation chemists calculate partition of dose by calculating the electron fraction in the components but with such different atomic numbers as Pu ($Z = 94$) and H ($Z = 1$) that is not appropriate, because from the Bethe equation it is average ionisation potential which is important and there is considerable shielding of inner electrons in Pu. The dose partition can be calculated using the Bethe equation but a simpler process is just to consider stopping powers in water and PuO_2 using SRIM [14], and it can be shown that on a mass basis H_2O is 3.4 times as efficient as PuO_2 at stopping helium ions, thus:

$$\text{The dose in water} = \text{total dose emitted by } PuO_2 \times \frac{\text{wt water} \times 3.4}{\text{wt } PuO_2 + H_2O} \quad (2)$$

This approach removes the effect of different specific activities of the oxides and allows comparison with other hydrogen yields.

4.2. PuO_2 GH_2 values

GH_2 *vs.* monolayer coverage of H_2O is plotted in Fig. 3. This shows significantly higher GH_2 for "Magnox" material which

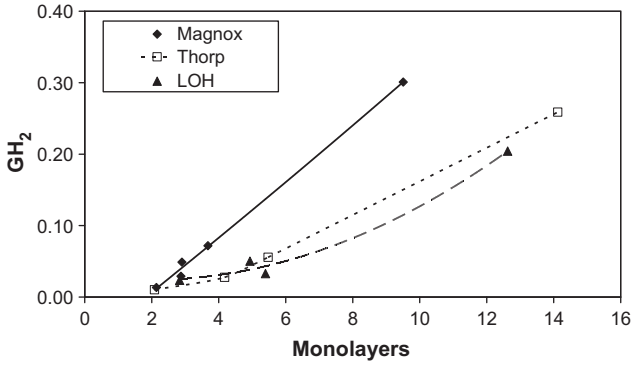

Fig. 3. H_2 *G*-values (molec. 100 eV^{-1}) *vs.* number of calculated monolayers of water for Magnox, Thorp and low SSA ("LOH") PuO_2 samples (note: assumes two monolayers still present after room temperature drying in desiccators).

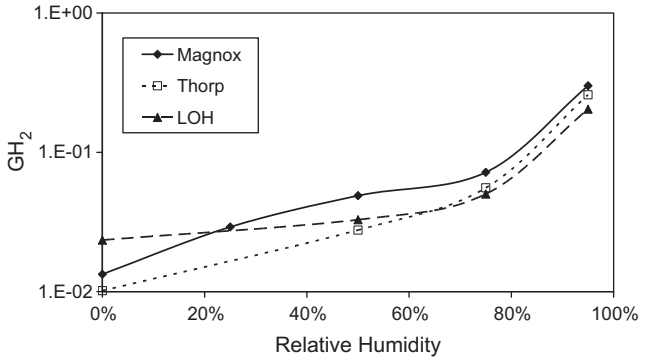

Fig. 4. H_2 *G*-values (molec. 100 eV^{-1}) *vs.* Relative Humidity (%) for Magnox, Thorp and low SSA ("LOH") PuO_2 samples.

seems unlikely but it is a consequence of the lower number of monolayers on "Magnox" PuO_2 compared with "Thorp" and ex-LOH material for a given RH (Fig. 1). Alternatively, if GH_2 is plotted *vs.* RH much better agreement is observed as shown in Fig. 4. This indicates that the number of monolayers is directly proportional to the RH and a conclusion from this is that either SSA or water mass is not well known or alternatively not all of the BET surface area is available for multi-monolayer adsorption of water (e.g. due to small pore sizes) for "Magnox" PuO_2. The important point, however, is that even at 95% RH, GH_2 is about a factor of 4–5 below the accepted value for bulk water (1.3 molec. 100 eV^{-1}). For comparison, the GH_2 values from the slurry experiments were $S = 0.53$ and $SN = 0.62$.

Alternatively, we can plot GH_2 (total dose) *vs.* RH in which GH_2 is calculated for total dose rather than the fraction in the water. This avoids any use of water mass or SSA but gives low results for ex-LOH PuO_2 due to its low SSA and therefore lower adsorbed water. Plotting GH_2 (total dose)/SSA *vs.* RH again gives a reasonable agreement between data (Fig. 5).

4.3. Comparison with data in the literature

It is also of interest to compare results from this work with other results from the literature which are shown in Fig. 6. In order to calculate the monolayers from water content, the SSA of Pu used in Livingstone and Duffey's work was obtained from Daniel [15]. The SSA of PuO_2 used by Vladimirova [5] has been derived from the stated calcination temperature using the correlation of Manchuron-Mandard and Madic [11] for SSA *vs.* calcination temperature although there is a wide spread in reported PuO_2 SSA

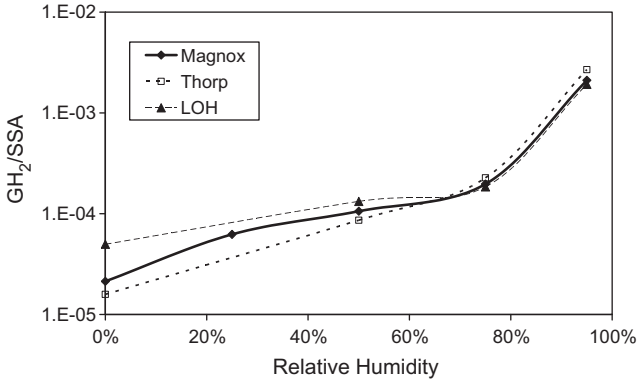

Fig. 5. H_2 *G*-values (molec. 100 eV^{-1}) for Magnox, Thorp and low SSA ("LOH") PuO_2 samples normalized for specific surface area variations plotted against Relative Humidity (%).

particularly when calcined below ~600 °C (see for example [16–18]). The data from Vladimirova [5] have been adjusted by assuming the excess H_2 measured over water added must have arisen from additional water. The data are rather scattered particularly below ~15 monolayers, probably reflecting the susceptibility of these data to factors such as variations in measured SSA, initial water content and experimental conditions. However, the figure clearly shows an increasing trend of GH_2 with the number of water monolayers or RH.

4.4. Radiolysis at a surface

It has been noted by several authors [19–21] that GH_2 values from water on the surfaces of some oxides including the rare earths and ZrO_2 are much higher than for bulk water (GH_2 > 100 molec. 100 eV^{-1}) and too high to have arisen from the fraction of energy in the water and so must arise from energy transfer from solid to aqueous phases. It should be noted that most of these studies were from gamma radiolysis. That clearly does not happen for PuO_2 where quite the opposite trend is observed. Decomposition of adsorbed water following energy transfer to an interface may be quite different to radiolysis of that adsorbed water which in turn may occur by a quite different mechanism to radiolysis of bulk water. The following are some of the key points concerning H_2 production at interfaces from the literature:

(1) In some cases energy transfer occurs and GH_2 is much greater than for bulk water.
(2) In some cases GH_2 is the same as bulk water.
(3) In some cases, in particular for Co_3O_4, Fe_2O_3, MnO_2 and CuO [21] GH_2 is less than bulk water. It is noteworthy that each of these oxides can be reduced. In these cases it is possible that energy transfer does not occur but alternatively it may occur but with no net effect. A possible reason is that decomposition products may recombine at the surface.
(4) Another possibility for PuO_2 is that energy transfer does not occur in a radiation damaged solid. No radiation damaged solids have been tested.
(5) Radiolysis of water at an interface may be quite different to bulk water in two respects: radiolysis of adsorbed water could be a different process giving different initial yields or the interface may essentially be a very efficient scavenger of the radicals normally produced from water decomposition. The diameter of a water molecule is about 3×10^{-8} cm so radicals can be formed adjacent to the surface or just a few hops to the surface; assuming a diffusion constant (D) of 10^{-5} cm^2 s^{-1} and taking the distance diffused x as $x = \sqrt{2Dt}$, then the time to diffuse to the surface through

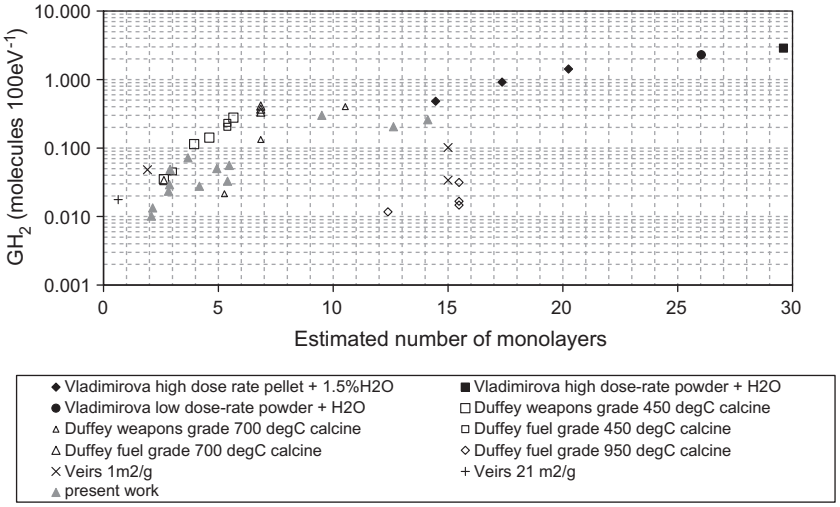

Fig. 6. Comparison of available data for H_2 *G*-value (molec. 100 eV^{-1}) plotted against the number of calculated water monolayers on PuO_2 (present work = grey closed triangles; data of Viers and co-workers [6] = cross symbols; data of Vladimirova and co-workers [5] = closed symbols; data of Duffey and co-workers [4] = open symbols. PuO_2 sources given in legend).

three monolayers (10^{-7} cm) is 5×10^{-10} s. We know from Buxton et al. [22] that several spinel oxides can be reductively dissolved by long lived radiolysis products, e.g. organic radicals, so Pu(IV) should react with H·, OH· and e^- especially considering that PuO_2 is known to react with Ag^{2+} and Cr^{2+} in oxidative and reductive dissolution [23]. Similar comments should apply to other oxides, e.g. the list in Ref. [21]. Some oxides, e.g. ZrO_2 and virtually all lanthanides, might be expected to be unreactive towards radiolysis products.

So, if the oxide surface contains redox-active metal ions, reaction between the surface and radicals produced from water decomposition after energy transfer would then not lead to excess hydrogen evolution. The low values of GH_2 with low water coverage for PuO_2 are in contrast to data for UO_2 and CeO_2, which have been considered as surrogates for PuO_2. Here, the opposite trend was reported – i.e. very large GH_2 in the first few monolayers. It is difficult to explain excess H_2 from UO_2 and CeO_2 but not PuO_2. UO_2 might be expected to have a layer of U_3O_8 on the surface but Icenhour [24] apparently did not see excess H_2 with U_3O_8. CeO_2 cannot be oxidised but can be reduced to Ce^{3+} so the excess H_2 might not be expected unless reduction of CeO_2 by H· and e^- is thermodynamically unlikely. CeO_2 can certainly be reduced by H_2 at around 470 K [25]. If decomposition by energy transfer can occur by a "molecular" mechanism then these anomalies can be explained but then the low H_2 from the list of oxides above are a problem unless decomposition of water does not occur on them because of e.g. low "band gaps". An alternative explanation for the difference between CeO_2 and PuO_2 is that Ce_2O_3 and Pu_2O_3 are both thermodynamically unstable with water [26] so although both CeO_2 and PuO_2 can be reduced, the sesquioxides will reduce water. However, in the case of PuO_2 the surface is known to contain Pu(V) from solubility studies [27] so it may be that this species is reduced and the resulting Pu(IV) would not reduce water to H_2. There is no equivalent Ce(V) species.

The energy deposition process in a few monolayers may be different from bulk water so that the concept of a "spur" and Linear Energy Transfer (LET) will not apply. Yields from alpha radiolysis in water are different to gamma radiolysis, because of the higher LET of alpha radiolysis but this cannot apply in a few monolayers because the result of high LET is spur overlap but it is questionable whether even one spur will form in a few monolayers. However it is almost certain that water is ionized by the passage of alpha particles so some of the initial processes for bulk water should apply (Eqs. (3)–(9)):

$$H_2O \rightarrow H_2O^+ + e^- \quad (3)$$

$$H_2O^+ + e^- \rightarrow H_2O^* \quad (4)$$

$$H_2O^+ + H_2O \rightarrow OH^\cdot + H_3O^+ \quad (5)$$

$$e^- + H_2O \rightarrow e^-_{aq} \quad (6)$$

$$H_2O^* \rightarrow H^\cdot + OH^\cdot \quad (7)$$

$$H_2O^* \rightarrow H_2 + O^\cdot \quad (8)$$

$$OH^\cdot + H_2 \rightarrow H^\cdot + H_2O \quad (9)$$

It is also questionable whether products from second order reactions will form because reactions of radiolysis products (e^-_{aq}, OH·) with the surface may dominate; this suggests reaction Eq. (8) is important.

Much of this is speculation at present because the processes in monolayers are not known, for example, whether a hydrated electron e^-_{aq} will form in proximity to an oxide surface. It is interesting in Fig. 6 that as the number of monolayers increases and some of the radiolysis products are formed further from the surface, then yields increase which can be explained if radicals are formed further from the surface and it becomes more like bulk water. It is also noteworthy that for this work at least there is a correlation with RH rather than monolayer coverage.

Reasons for differences or scatter in the data are not known, but in all this discussion the only surface adsorbate considered has been H_2O whereas, unless specifically excluded, PuO_2 will also contain CO_2 and NO_x which could have an impact on surface chemistry [28,29]. Ref. [29] reports time dependent adsorption of O_2 which is only recovered by desorption at elevated temperature accompanied by smaller quantities of CO_2. This strongly suggests a (thermal or radiation) chemical reaction but the nature of the product is unknown.

Regarding the slurry experiments, the ~17% increase in GH_2 with nitrite present is consistent with a H_2 removal reaction, e.g. Eq. (9) followed by Eq. (10). The difference suggests that similar

H_2 consumption reactions can occur on the surface of moist PuO_2. The ratio of yields of the slurry to that expected from a homogeneous (aqueous) solution is therefore 0.62/1.3 = 0.48. Simplistic estimates suggest this is equivalent to radiolysis of $\sim 10^5$ monolayers water coverage.

$$OH^{\cdot} + NO_2^- \rightarrow OH^- + NO_2 \quad (10)$$

4.5. Application to Pu storage canisters

Using the data from Table 3, it can be seen that the rate of production of H_2 from "dry" PuO_2 was about 10^{-5} cm^3 h^{-1} g PuO_2^{-1}. Although this figure is subject to considerable uncertainty it can be shown that for a nominal 7 kg can of PuO_2 this is equivalent to ~ 600 cm^3 of H_2 per year which, assuming a gas volume in the can of 4 dm^3, is equivalent to 0.15 bar per year. As there is no sign of pressurisation at these rates under normal storage conditions, then it must be concluded that there is an efficient removal mechanism.

4.6. Thermal vs. radiolytic mechanisms

There has been debate as to whether H_2 is formed *via* a radiolytic or thermal mechanism with the claim [9] that there is a reaction:

$$PuO_2 + H_2O \rightarrow PuO_{2+x} + H_2 \quad (11)$$

However, the proposal has been dismissed on thermodynamic grounds [27] and it can be seen from data in this report that the rate of H_2 production is quite clearly dependent on water content and only becomes significant above $\sim$4 monolayers. It is highly unlikely that a thermal reaction with water at the PuO_2 surface would be dependent on more than the chemisorbed and first physisorbed layers. Secondly, it can be seen from this work and to a lesser extent from [4] that the H_2 production rate is dependent on dose rate which is not consistent with a thermal reaction. However, if the above discussion is correct and reactions of radicals with the surface can occur then production of H_2 could be accompanied by oxidation of the PuO_2 surface:

$$PuO_2 + OH^{\cdot} \rightarrow PuO_2OH \quad (12)$$

5. Conclusions

H_2 production rates from three different samples of Sellafield production line PuO_2 across a range of humid atmospheres have been measured. The results confirm the low production rates at low water monolayer coverage, increasing sharply between 75% and 95% RH. These data show that the amount of hydrogen produced is dependent on the number of monolayers or RH and the specific activity of the PuO_2. These preliminary observations demonstrate that in our experiments H_2 production is a radiolytic rather than thermal process. Simple estimations based on hydrogen generation rates measured here indicate that there must be recombination reactions occurring within cans of PuO_2 that inhibit pressurisation under most storage conditions. An interesting observation is the higher H_2 production rate from "Magnox" PuO_2, which is of a lower specific activity than the "Thorp" Pu, this may be related to the higher SSA and porosity.

Whilst our data fit trends from the literature the overall scatter in the data is unsatisfactory. However, it is clear that hydrogen production will be affected by a number of factors including the number of monolayers of water and the presence of other adsorbates (e.g. NO_x and CO_2). Further work is now needed to reduce sources of uncertainty in these data and confirm the trends observed, particularly the factors that suppress H_2 generation close to the surface of the PuO_2.

Acknowledgments

We thank the UK Nuclear Decommissioning Authority for funding this work through the Direct Research Portfolio and Sellafield Ltd. for provision of plutonium oxide. Pu isotopic analyses were made by Sellafield Analytical Services and NNL Analytical Team.

References

[1] Department of Energy and Climate Change, Management of the UK's Plutonium Stocks. A Consultation Response on the Long-Term Management of UK-Owned Separated Civil Plutonium, Department of Energy & Climate Change, London, 2011.
[2] P. Gilchrist, Plutonium Strategy, Current Position Paper, SMS/TS/B1-PLUT/001/A, Nuclear Decommissioning Authority, 2011 <http://www.nda.gov.uk>.
[3] DOE Standard: Stabilization, Packaging, and Storage of Plutonium-Bearing Materials, DOE-STD-3013-2012, Washington, DC, 2012.
[4] J.M. Duffey, R.R. Livingston, Gas Generation Testing of Plutonium Dioxide, WSRC-MS-2002-00705, Westinghouse Savannah River Company, 2002.
[5] M.V. Vladimirova, Radiochemistry 44 (2002) 501–507.
[6] D.K. Veirs, Mater. Res. Soc. Symp. Proc. 893 (2006). 0893-JJ07-03.1–03.6.
[7] D.J. Hodkin, R.S. Pitman, P.G. Mardon, Gas Evolution from Solid Plutonium Bearing Residues During Storage, AERE-M 1644, Harwell, 1965.
[8] J.M. Haschke, J.L. Stakebake, Handling, storage and disposition of plutonium and uranium, in: L.R. Morss, N.M. Edelstein, J. Fuger (Eds.), The Chemistry of the Actinide and Transactinide Elements, third ed., vol. 5, Springer, Dordrecht, 2006, pp. 3199–3272 (Chapter 28).
[9] J.M. Haschke, R.G. Haire, Crystalline solids and corrosion chemistry, in: D.C. Hoffman (Ed.), Advances in Plutonium Chemistry 1967–2000, American Nuclear Society, La Grange Park, 2002, pp. 212–255 (Chapter 9).
[10] C. Ronchi, J.P. Hiernaut, J. Nucl. Mater. 325 (2004) 1–12.
[11] X. Manchuron-Mandard, C. Madic, J. Alloys Comp. 235 (1996) 216–224.
[12] J.L. Stakebake, L.M. Steward, J. Colloid Interface Sci. 42 (1973) 328–333.
[13] D.R. Lide (Ed.), Handbook of Chemistry and Physics, CRC Press Inc., Boston, 1992, pp. 15.18–15.21.
[14] J.F. Ziegler, SRIM – The Stopping and Range of Ions in Matter, 2013, see <http://www.srim.org/>.
[15] W.E. Daniel, Literature Review of PuO_2 Calcination Time and Temperature Data for Specific Surface, Area, SRNL-TR-2011-00334, 2012.
[16] K.E. Francis, R.G. Sowden, The Microstructure of Plutonium Dioxide Prepared by Various Methods, AERE-R-2939, Harwell, 1959.
[17] J.D. Moseley, R.O. Wing, Properties of Plutonium Dioxide, Rocky Flats, RFP-503, US-DOE, 1965.
[18] J.M. Haschke, T.E. Ricketts, Plutonium Dioxide Storage: Conditions for Preparation and Handling, LA-12999-MS, Los Alamos National Laboratory, 1995.
[19] J.A. LaVerne, L. Tandon, J. Phys. Chem. B 107 (2003) 13623–13628.
[20] J.A. LaVerne, L. Tandon, J. Phys. Chem. B 106 (2002) 380–386.
[21] N.G. Petrik, A.B. Alexandrov, A.I. Vall, J. Phys. Chem. B 105 (2001) 5935–5944.
[22] G.V. Buxton, D.W. Cartmell, R.M. Sellers, J. Chem. Soc. Farad. Trans. I (85) (1989) 3513–3528.
[23] C. Madic, P. Berger, X. Manchuron-Mandard, Mechanisms of the rapid dissolution of plutonium dioxide in acidic media under oxidizing or reducing conditions, in: L.R. Morss, J. Fuger (Eds.), Transuranium Elements: A Half Century, American Chemical Society, Washington, DC, 1992, pp. 457–468 (Chapter 44).
[24] A.S. Icenhour, L.M. Toth, H. Luo, Water Sorption and Gamma Radiolysis Studies for Uranium Oxides, ORNL/TM-2001/59, Oak Ridge National Laboratory, Tennessee, 2002.
[25] A. Laachir, V. Perrichon, A. Badri, J. Lamotte, E. Catherine, J.C. Lavalley, J. El Fallah, L. Hilaire, F. Le Normand, E. Quéméré, G.N. Sauvion, O. Touret, L. Chem. Soc. Farad. Trans. 87 (1991) 1601–1609.
[26] P. Franke, D. Neuschütz (Eds.), Landolt Bornstein: Numerical Data and Functional Relationships in Science and Technology Group IV: Physical Chemistry. Thermodynamic Properties of Inorganic Materials Compiled by SGTE, Pure substances, vol. 19, subvol. A, Springer, Berlin, 1999.
[27] V. Neck, M. Altmaier, T. Fanghänel, C.R.Chimie 10 (2007) 959–977.
[28] I.G. Jones, D. Darke, Thermal Desorption Behaviour of Plutonium Dioxide, AERE-R-11222, Harwell, 1984.
[29] I.G. Jones, The Adsorptive Behaviour of Plutonium Dioxide on Exposure to Argon, Nitrogen, Oxygen and Air, AERE-R-11383, Harwell, 1985.